# Electronic Supplementary Information

## Ultrasensitive determination of ascorbic acid by using cobalt oxyhydroxide nanosheet to enhance the chemiluminescence of luminol-H₂O₂ system

Huihui Xu,[a] Qiyong Cai,[a] Qiuyu Nie,[a] Zhun Qiao,[a] Song Liu*[a] and Zhaohui Li*[b]

[a] *Institute of Chemical Biology and Nanomedicine (ICBN), State Key Laboratory of Chemo/ Biosensing and Chemometrics, College of Chemistry and Chemical Engineering, Hunan University, Changsha, 410082, P. R. China*

[b] *College of Chemistry and Molecular Engineering, Zhengzhou University, Zhengzhou 450001, P. R.China*

* Corresponding authors. Tel.: +86-731-88822568.

E-mail address: liusong@hnu.edu.cn (S. Liu), zhaohui.li@zzu.edu.cn (Z. H. Li),
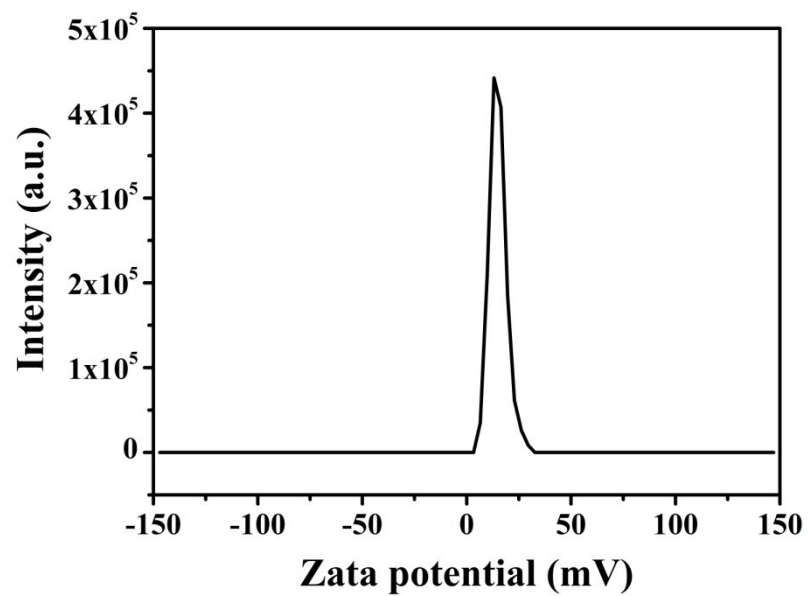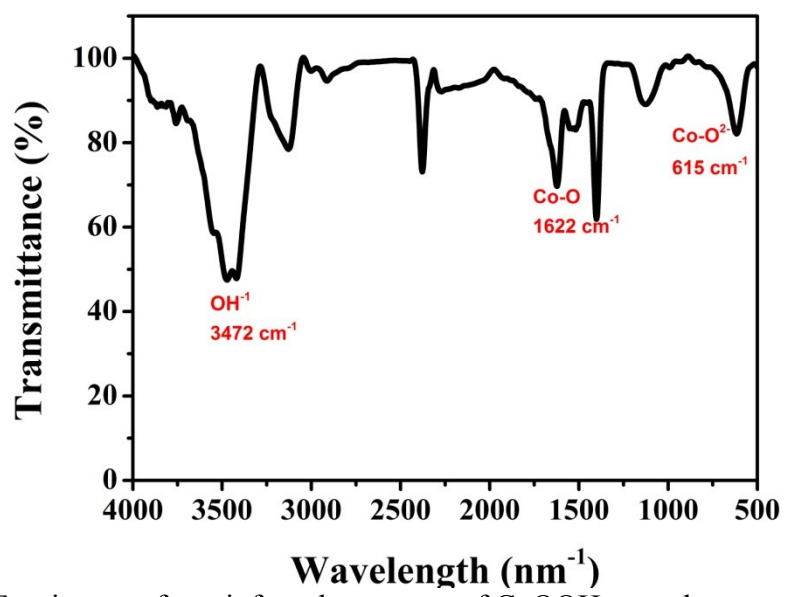
**Fig. S1.** Zata potential of CoOOH nanosheets.

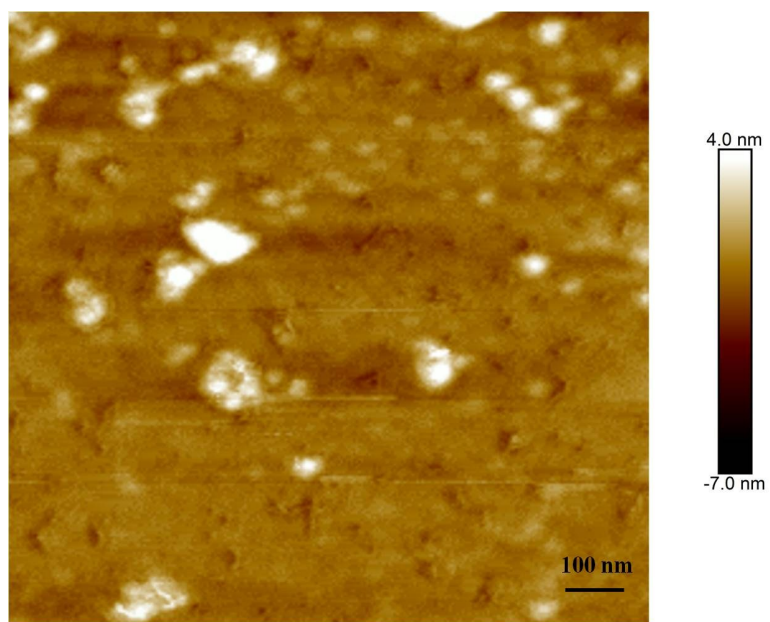**Fig. S2.** Fourier transform infrared spectrum of CoOOH nanosheets.

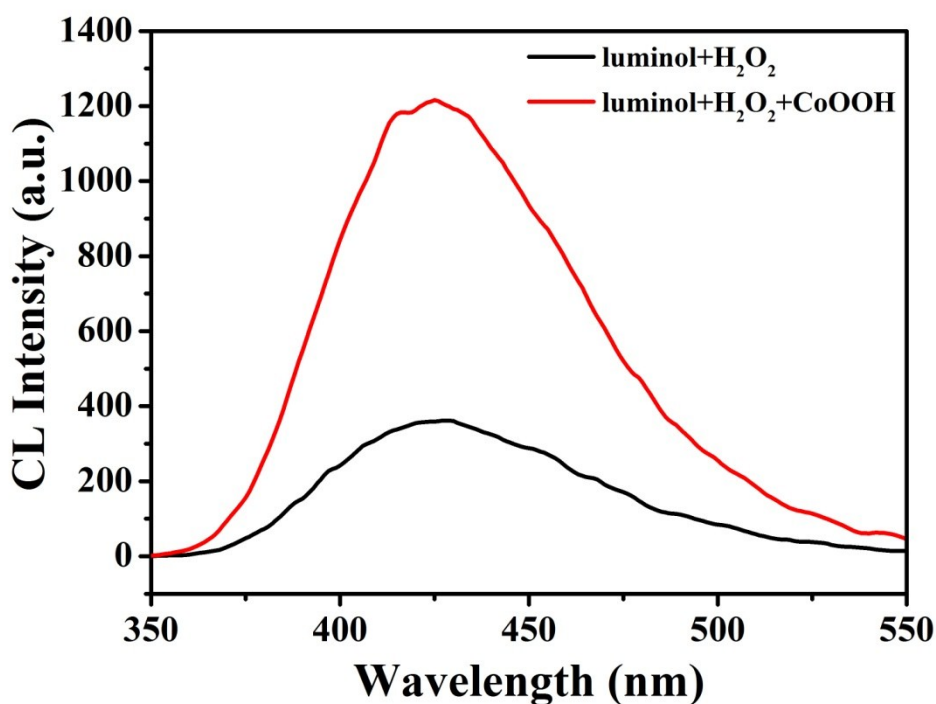**Fig. S3.** AFM image of CoOOH nanosheets

**Fig. S4.** CL spectra of luminol-$H_2O_2$ system and luminol-$H_2O_2$-CoOOH system. The concentration of luminol, $H_2O_2$ and CoOOH is $10^{-4}$ mol·$L^{-1}$, $10^{-2}$ mol·$L^{-1}$, $5 \times 10^{-7}$ g/mL respectively.

From Fig S4 we can observed that the CoOOH nanosheet enhanced effect is not as good as the description in the manuscript. There are two causes can explain this phenomenon. On the one hand, the CL spectra measurements needs to manual operation, the CL intensity is reduced due to the time delay in this process. On the other hand, the sensitivity of fluorescence spectrometer is much lower than microplate reader.
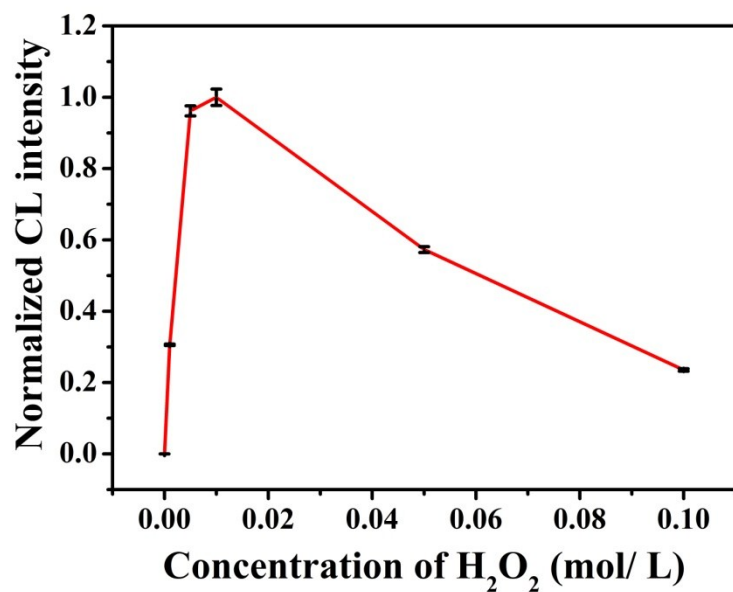
**Fig. S5.** Effect of $H_2O_2$ concentration on CL intensity of the CoOOH enhanced luminol–$H_2O_2$ CL system: luminol, $10^{-4}$ mol·$L^{-1}$; Tris-HCl, 10 mmol·$L^{-1}$; pH 10; CoOOH, $5 \times 10^{-7}$ g/mL; flow velocity, pump A: 200 μL/s; pump B: 200 μL/s. The error bar represents standard deviation of three replicate measurements.

**Fig. S6.** Effect of CoOOH concentration on CL intensity of the CoOOH enhanced luminol–$H_2O_2$ CL system: luminol, $10^{-4}$ mol·$L^{-1}$; $H_2O_2$, 0.01 mol·$L^{-1}$; Tris-HCl, 10 mmol·$L^{-1}$; pH 10; flow velocity, pump A: 200 μL/s; pump B: 200 μL/s. The error bar represents standard deviation of three replicate measurements.

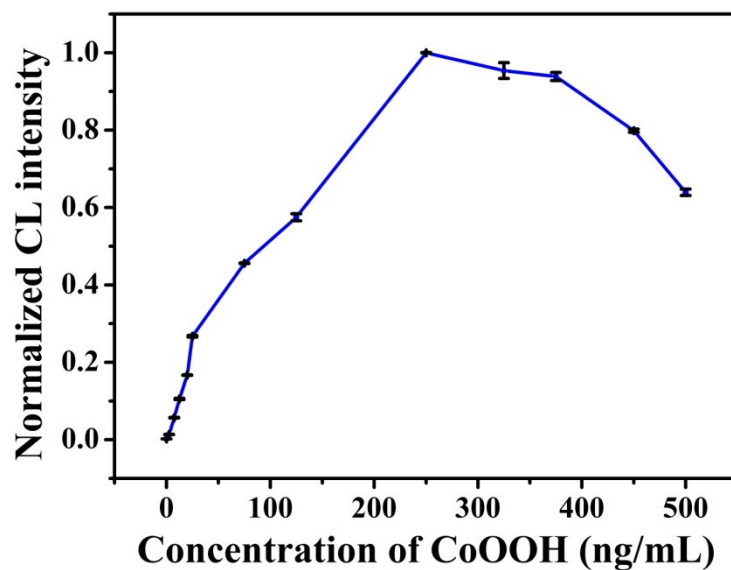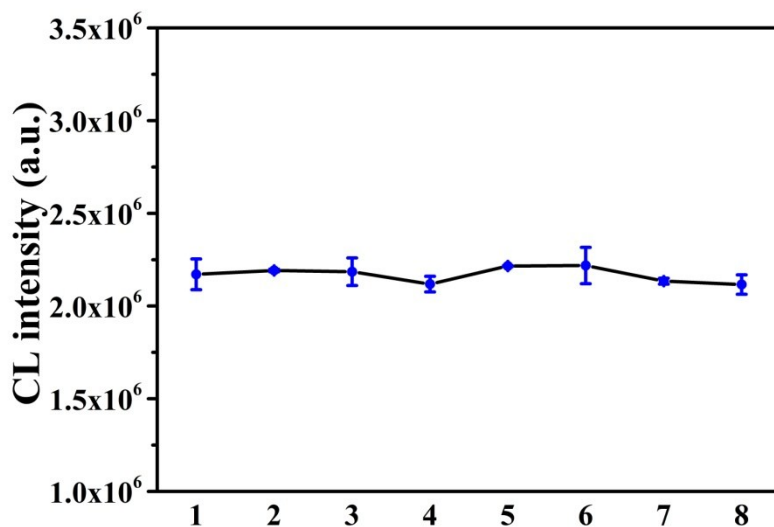**Fig. S7.** Effect of flow velocity on CL intensity of the CoOOH enhanced luminol–$H_2O_2$ CL system: luminol, $10^{-4}$ mol·L$^{-1}$; $H_2O_2$, 0.01 mol·L$^{-1}$; Tris-HCl (10 mmol·L$^{-1}$); pH 9.5; CoOOH, $2.5 \times 10^{-7}$ g/mL (1: pump A:100 μL/s, pump B: 200 μL/s; 2: pump A:150 μL/s, pump B: 200 μL/s; 3: pump A:200 μL/s, pump B: 200 μL/s; 4: pump A:250 μL/s, pump B: 200 μL/s; 5: pump A: 200 μL/s, pump B: 100 μL/s; 6: pump A: 200 μL/s, pump B: 150 μL/s; 7: pump A: 200 μL/s, pump B: 200 μL/s; 8: pump A:200 μL/s, pump B: 250 μL/s). The error bar represents standard deviation of three replicate measurements.

**Table S1:** Comparision of different methods for AA determination.

| Method | System | Range (nmol·L$^{-1}$) | LOD (nmol·L$^{-1}$) | Reference |
|---|---|---|---|---|
| Fluorescence turn-on probe | GQDs–Cu(II) | $3.0\times10^2$-$1.0\times10^4$ | 94 | 1 |
| Fluorescence turn-off sensor | BSA–Au NCs | $1.5\times10^3$-$1.0\times10^4$ | 200 | 2 |
| Ratiometric nanosensor | CdTe QDs–KMnO$_4$ | $3\times10^2$-$1.0\times10^4$ | 74 | 3 |
| Fluorescence turn-on nanoprobe | TPNPs–CoOOH[1] | $1\times10^3$–$2.0\times10^4$ | 170 | 4 |
| Turn-on fluorescent probe | C-Dots–MnO$_2$ | $5\times10^2$-$2.0\times10^4$ | 68 | 5 |
| Ratiometric Fluorescent | NIR-based DEFN[2] | $0$-$5.0\times10^6$ | 610 | 6 |
| Colorimetry | Mesoporous silica-coated gold nanorods | $1\times10^2$-$2.5\times10^3$ | 49 | 7 |
| Colorimetric sensor | MnO$_2$ nanosheets | $5\times10^2$-$1.0\times10^4$ | $1.0\times10^3$ | 8 |
| Flow injection-chemiluminescence determination | Luminol–K$_3$Fe(CN)$_6$–GNPs | $1\times10^{-1}$ -$1\times10^3$ | 0.02 | 9 |
| Chemiluminescence determinatioon | Luminol–H$_2$O$_2$–GMs[3] | $1$-$1.0\times10^4$ | 0.35 | 10 |
| Flow injection-chemiluminescence | Luminol–H$_2$O$_2$–cation exchange resin | $2.0\times10^1$-$6\times10^2$ | 6.03 | 11 |
| Chemiluminescence detection | NaHCO$_3$–H$_2$O$_2$–CdSe/CdS QDs | $1\times10^2$-$1.0\times10^5$ | 6.7 | 12 |
| Chemiluminescence detection | Luminol–H$_2$O$_2$–CoOOH | $1\times10^{-3}$ - $5\times10^{-1}$ | $3.9\times10^{-4}$ | This work |

[1]TPNPs, two-photon nanoparticles

[2] DEEN, dual-emission fluorescent nanohybrid

[3] GMs, GO@HKUST-1

**Reference**

1    J. Liu, Z. Chen, D. Tang, *et al.* Graphene quantum dots-based fluorescent probe for turn-on sensing of ascorbic acid, *Sens. Actuators, B: Chem.*, 2015, 212, 214-219.

2    X. Wang, P. Wu, X. Hou, *et al.* An ascorbic acid sensor based on protein-modified Au nanoclusters, *Analyst*, 2013, 138, 229-233.

3    S. Huang, F. Zhu, Q. Xiao, *et al.* A CdTe/CdS/ZnS core/shell/shell QDs-based "OFF–ON" fluorescent biosensor for sensitive and specific determination of l-ascorbic acid, *RSC Adv.*, 2014, 4, 46751-46761.

4    H. Meng, X. Zhang, C. Yang, *et al.* Efficient two-Photon fluorescence nanoprobe for turn-On detection and imaging of ascorbic acid in living cells and tissues, *Anal .Chem.*, 2016, 88, 6057-6063.

5    Y. Hu, L. Zhang, X. Geng, *et al.* A rapid and sensitive turn-on fluorescent probe for ascorbic acid detection based on carbon dots–$MnO_2$ nanocomposites, *Anal. Methods.*, 2017, 9, 5653-5658.

6    P. Zhao, K. He, Y. Han, *et al.* Near-infrared dual-emission quantum dots-gold nanoclusters nanohybrid via co-template synthesis for ratiometric fluorescent detection and bioimaging of ascorbic acid in vitro and in vivo, *Anal. Chem.*, 2015, 87 9998-10005.

7    G. Wang, Z. Chen, L. Chen, Mesoporous silica-coated gold nanorods: towards sensitive colorimetric sensing of ascorbic acid via target-induced silver overcoating, *Nanoscale*, 2011, 3, 1756-1759.

8    Z. Huang, Q. Cai, D. Ding, *et al.* A facile label-free colorimetric method for highly sensitive glutathione detection by using manganese dioxide nanosheets, *Sens. Actuators, B: Chem.*, 2017, 242, 355-361.

9    Y. Dong, T. Gao, X. Chu, *et al.* Flow injection-chemiluminescence determination of ascorbic acid based on luminol–ferricyanide–gold nanoparticles system, *J. Lumin.*, 2014, 154, 350-355.

10   Q. Zhu, D. Dong, X. Zheng, *et al.* Chemiluminescence determination of ascorbic acid using graphene oxide@copper-based metal–organic frameworks as a catalyst, *RSC Adv.*, 2016, 6, 25047-25055.

11  L. Cai, C. Xu, An automated method for determination of ascorbic acid in urine by flow injection chemiluminescence coupling with on-line removal of interference, *J. Chil. Chem.Soc.*, 2011, 56.4, 938-940.

12  H. Chen, R. Li, L. Lin, *et al.* Determination of L-ascorbic acid in human serum by chemiluminescence based on hydrogen peroxide-sodium hydrogen carbonate-CdSe/CdS quantum dots system, *Talanta* , 2010, 81, 1688-1696.